Nonlinear hypocentre determination in the 3-D Western Bohemia a priori velocity model

Václav Bucha & Luděk Klimeš

Department of Geophysics
Faculty of Mathematics and Physics
Charles University in Prague

SW3D meeting

June 15-16, 2015

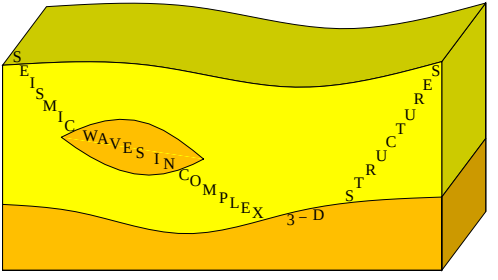

Outline

- **Introduction**
- **Nonlinear hypocentre determination**
- **Velocity model**
- **Measured data**
- **Hypocentres**

Introduction

- **During years 1998–1999, Luděk Klimeš prepared the numerical algorithm of a simplified version of the nonlinear hypocentre determination which takes into account the inaccuracy of the velocity model.**
- **The testing version of the corresponding code was included in the SW3D software in the year 2000.**
- **Recently, P. Bulant & L. Klimeš wrote down the theory underlying the numerical algorithm in their paper "Nonlinear hypocentre determination", and tested the numerical algorithm on a set of natural microearthquakes.**
- **We present completed old unpublished manuscript "Nonlinear hypocentre determination in the 3–D Western Bohemia a priori velocity model"**

- **with the description of the numerical algorithm of the simplified version of the nonlinear hypocentre determination,**
- **and with a simple demonstration of the algorithm on four local earthquakes in the seismically active part of Western Bohemia.**

Nonlinear hypocentre determination

- **The nonlinear hypocentre determination is composed of two main steps.**
- **The first step consists in computing theoretical travel times in the 3–D velocity model at the nodes of a dense rectangular grid covering the region where the hypocentre is searched for.**
- **In the second step, we use the theoretical travel times, their standard deviations, measured arrival times and their standard deviations for the determination of the nonnormalized 3–D marginal a posteriori density function which describes the relative probability of the seismic hypocentre.**

- **The numerical algorithm of hypocentre determination is based on the equations summarized by Bulant & Klimeš (2015, sec. 2).**

Velocity model

- **As the velocity model, we use the Western Bohemia a priori model, which was described in detail by Klimeš (1995), who created it manually as the initial velocity model for the iterative inversion of travel times from refraction seismic measurements.**
- **We do not know the accuracy of the 3–D Western Bohemia a priori velocity model. We thus substitute the correct standard deviations of theoretical travel times with the standard deviations corresponding to the 1–D mean model of the region by Klimeš (2002b, eq. 59).**

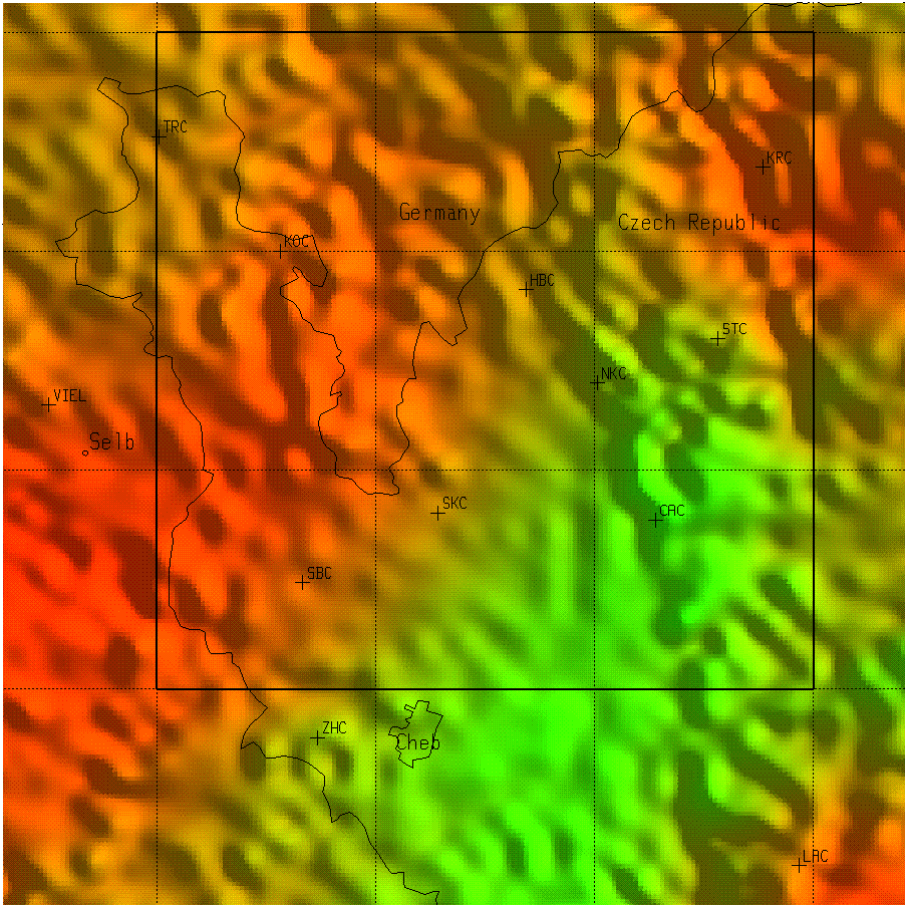

Part of the Western Bohemia a priori velocity model with the receivers and surface P wave velocities (the shadows are caused by the topography). Values of the velocity increase from **green** to **red** colour. The thick line rectangle limits the location grid, 30 × 30 km, depth is 17 km. The grid step is 0.5 km in all three directions. Receivers HBC and STC are not considered.

Measured data

- **The hypocentre determination code is tested by determining hypocentres of four local earthquakes recorded on January 1997 by the WEBNET local seismic network and one receiver in Germany.**
- **Three tested local earthquakes were measured by 10 receivers and one event was recorded by 6 receivers.**

receiver	*event 1*	*event 2*	*event 3*	*event 4*
CAC–Částkov	30.168	45.100	59.812	21.292
KOC–Kopaniny	31.316	46.228	60.972	22.788
KRC–Kraslice	30.856	45.804	60.484	22.292
LAC–Lazy	32.720	47.656	62.340	
NKC–Nový Kostel	29.856	44.748	59.512	21.060
SBC–Seeberg	31.472	46.372	61.108	22.672
SKC–Skalná	30.484	45.376	60.140	21.636
TRC–Trojmezí	32.432	47.352	62.072	
VIEL–Viel	32.672	47.584	62.312	
ZHC–Zelená Hora	32.132	47.036	61.768	

Hypocentres

- **For each event, the maximum $\sigma_{\mathrm{P3}}^{\max}$ of the nonnormalized 3–D marginal a posteriori density function which describes the relative probability of the seismic hypocentre, and arrival–time misfit y:**

event	$\sigma_{\mathrm{P3}}^{\max}$	y
1	0.569	1.126
2	0.686	0.754
3	0.605	1.007
4	0.908	0.193

- **We observed much greater uncertainty of the hypocentral position of event 4 determined just from six P–wave arrival times.**
- **We observed that the location of the maximum value of the nonnormalized 3–D marginal a posteriori density function may considerably differ from the mean hypocentre location given by the nonnormalized 3–D marginal a posteriori density function.**
- **Moreover, the mean hypocentre location often considerably depends on the dimensions of the location grid.**

Seismically active region of Western Bohemia. The thick line rectangle limits the location grid. Four approximately elliptical curves limit the regions where the probability density functions of the four epicentres exceed 10% of the respective maximum values.

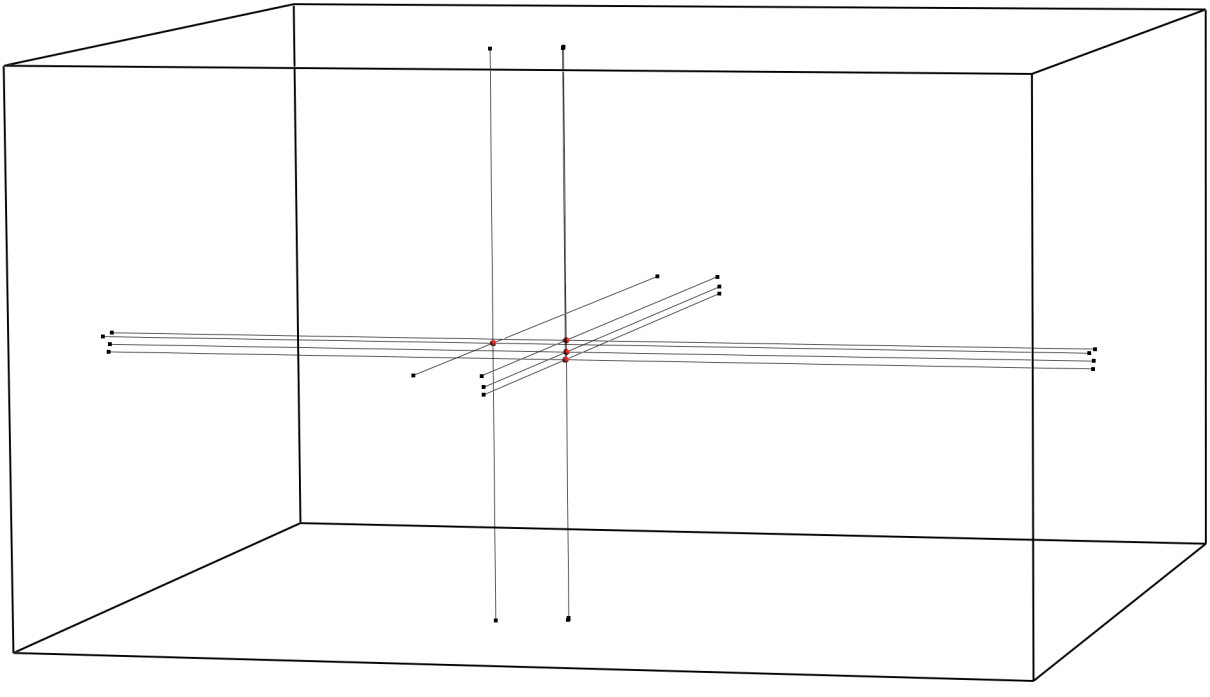

The locations of the centres of small cubes which are displayed as yardsticks (small **red** spheres), together with their projections onto the sides of the grid used for the nonlinear hypocentre determination. The displayed dimensions of the grid used for the nonlinear hypocentre determination are $30\,\mathrm{km}\times30\,\mathrm{km}\times17\,\mathrm{km}$.

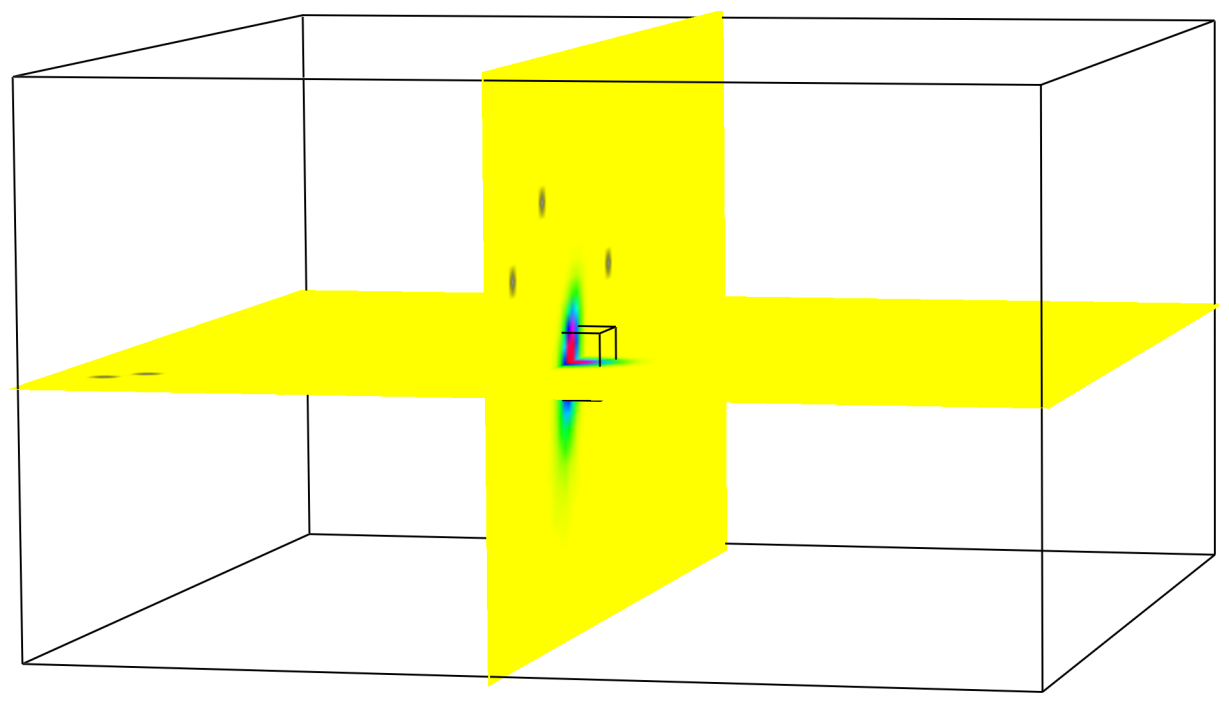

Nonnormalized 3–D marginal a posteriori density function of **event 1** determined using **10** P–wave arrival times. The zero values are displayed in **yellow**. The nonzero values range through **green**, **cyan**, **blue** and **magenta** to the maximum value displayed in **red**. The undefined values are displayed in **gray**, and denote the gridpoints at which at least one theoretical travel time is missing. The small cube has the sides of 2 km.

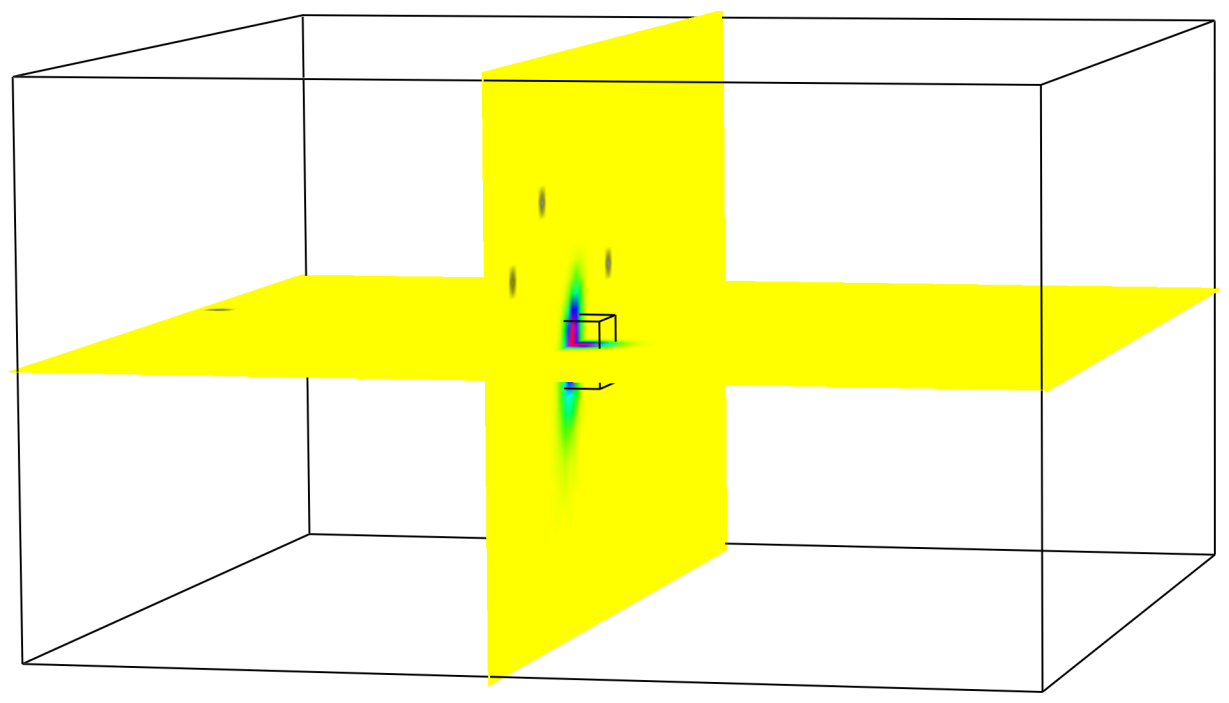

Nonnormalized 3–D marginal a posteriori density function of **event 2** determined using **10** P–wave arrival times. The zero values are displayed in **yellow**. The nonzero values range through **green**, **cyan**, **blue** and **magenta** to the maximum value displayed in **red**. The undefined values are displayed in **gray**, and denote the gridpoints at which at least one theoretical travel time is missing. The small cube has the sides of 2 km.

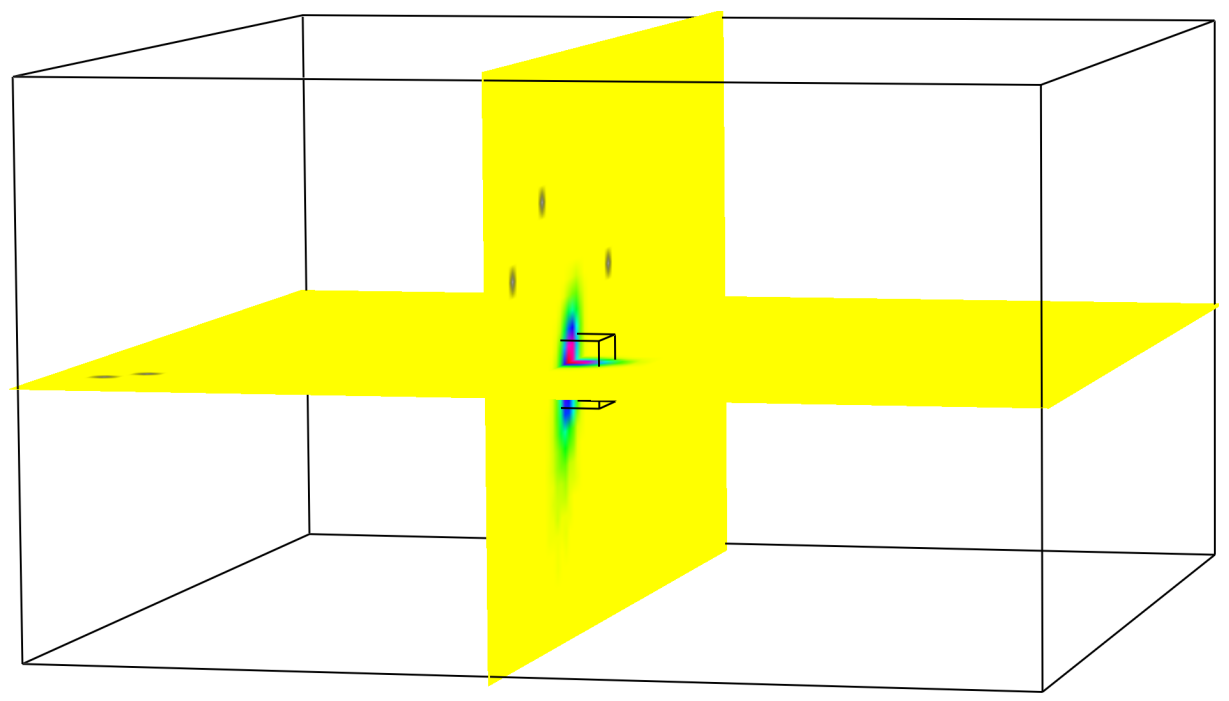

Nonnormalized 3–D marginal a posteriori density function of **event 3** determined using **10** P–wave arrival times. The zero values are displayed in **yellow**. The nonzero values range through **green**, **cyan**, **blue** and **magenta** to the maximum value displayed in **red**. The undefined values are displayed in **gray**, and denote the gridpoints at which at least one theoretical travel time is missing. The small cube has the sides of 2 km.

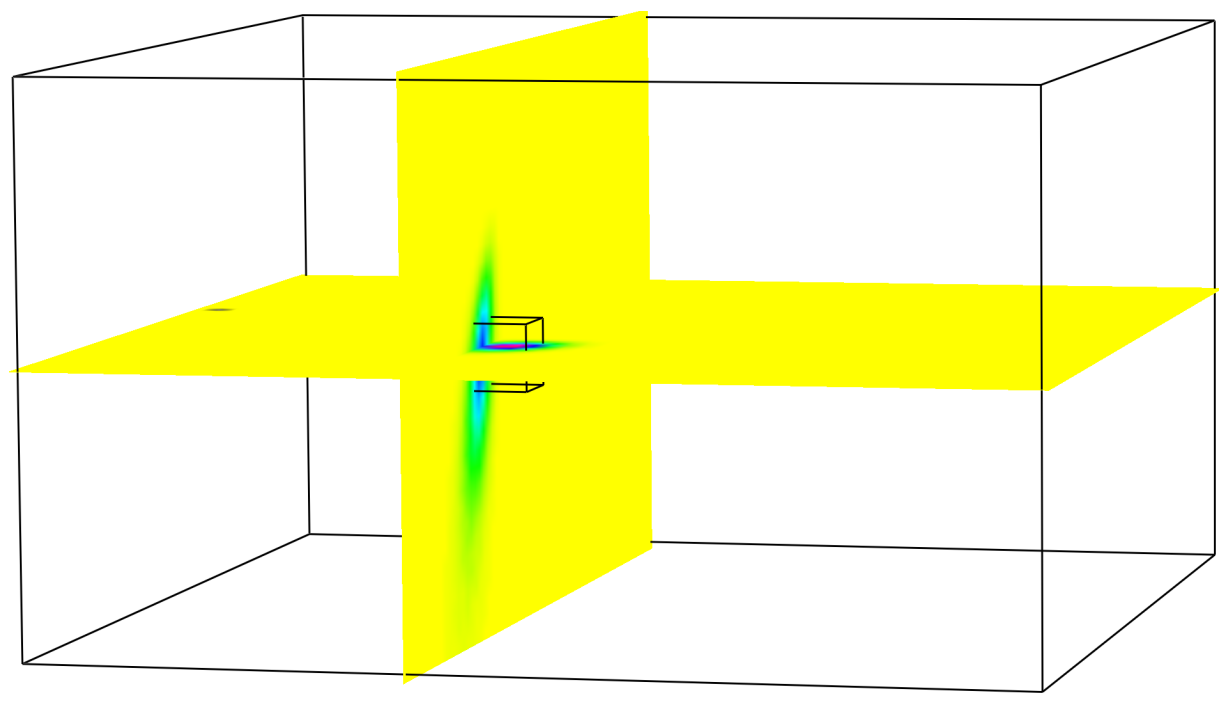

Nonnormalized 3–D marginal a posteriori density function of **event 4** determined using **6** P–wave arrival times. The zero values are displayed in **yellow**. The nonzero values range through **green**, **cyan**, **blue** and **magenta** to the maximum value displayed in **red**. The undefined values are displayed in **gray**, and denote the gridpoints at which at least one theoretical travel time is missing. The small cube has the sides of 2 km.

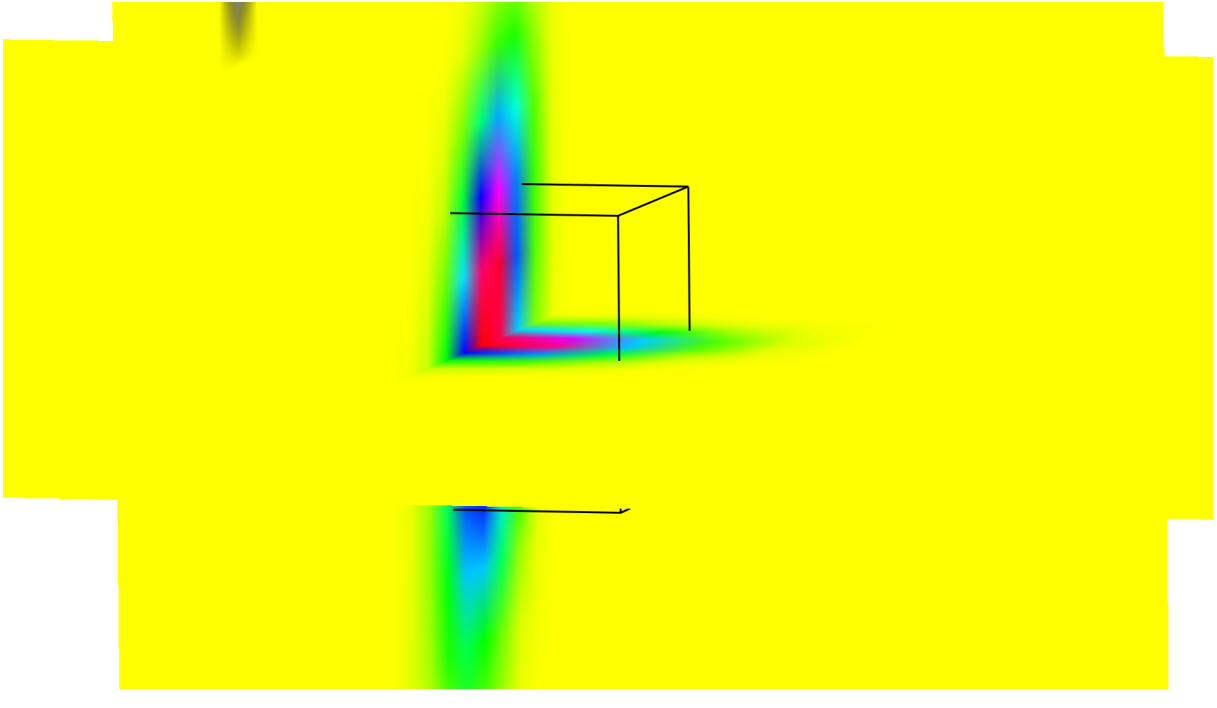

The detail of the interpolated discretized nonnormalized 3–D marginal a posteriori density function of **event 1**, displaying the hypocentral region. The cube has the sides of 2 km.

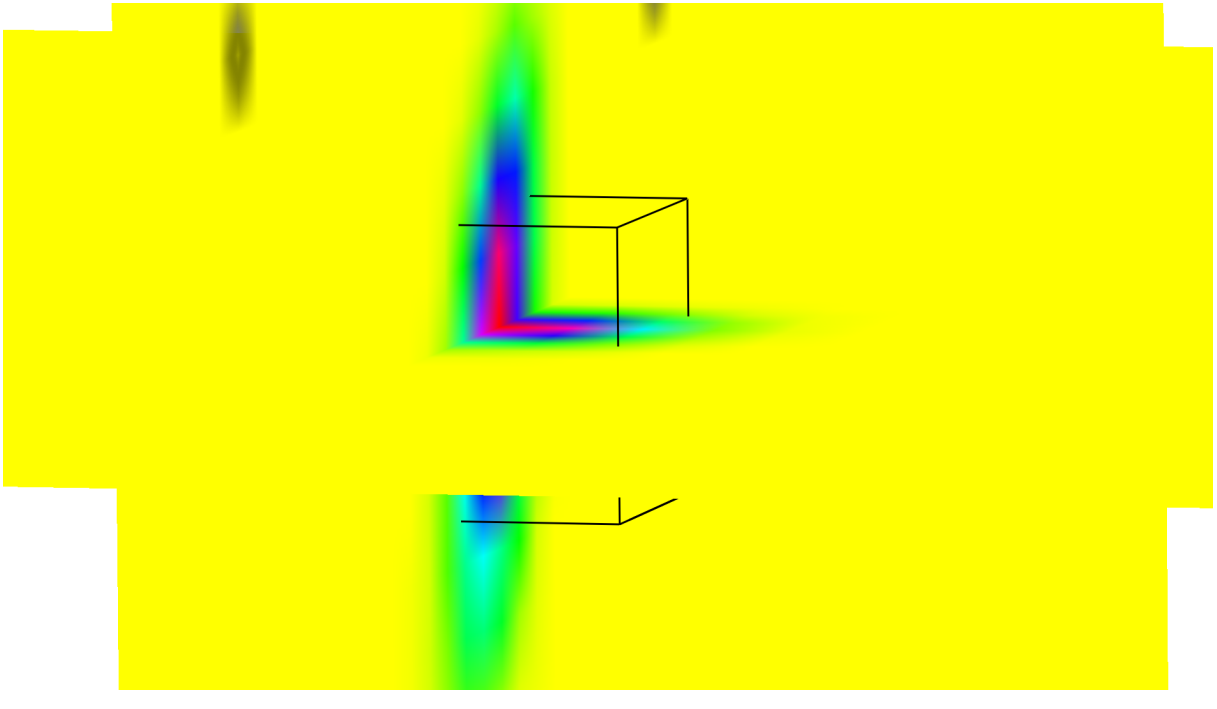

The detail of the interpolated discretized nonnormalized 3–D marginal a posteriori density function of **event 2**, displaying the hypocentral region. The cube has the sides of 2 km.

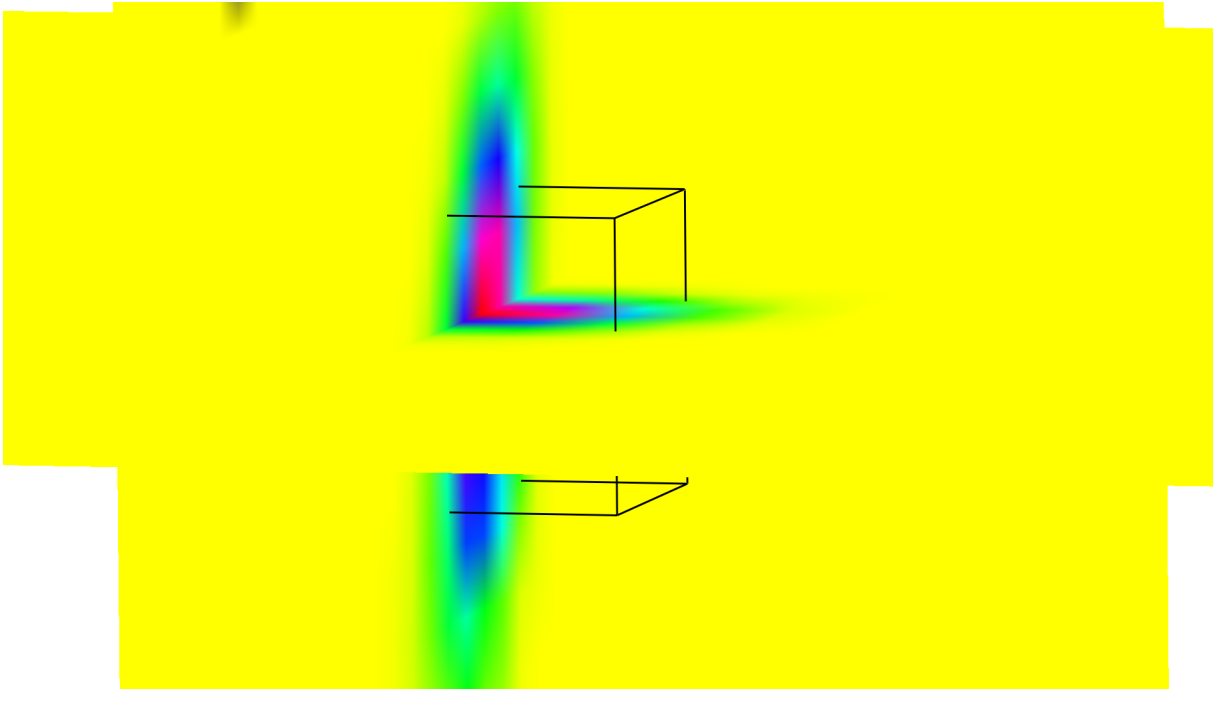

The detail of the interpolated discretized nonnormalized 3–D marginal a posteriori density function of **event 3**, displaying the hypocentral region. The cube has the sides of 2 km.

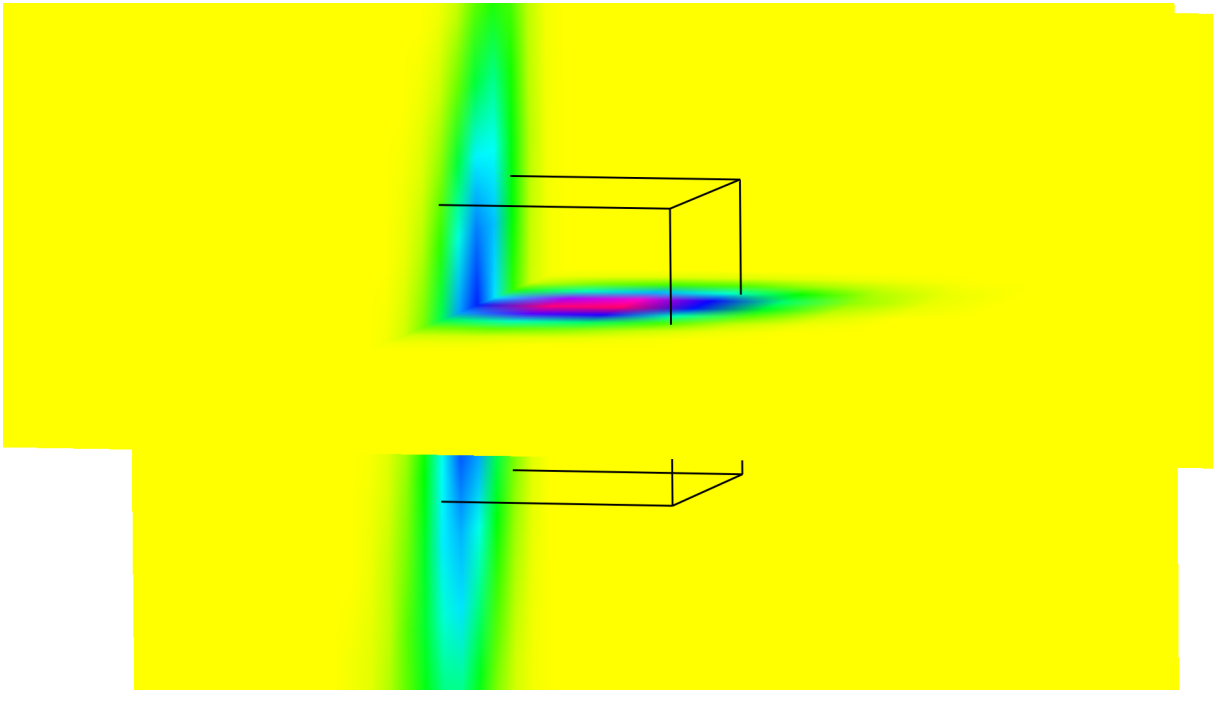

The detail of the interpolated discretized nonnormalized 3–D marginal a posteriori density function of **event 4**, displaying the hypocentral region. The cube has the sides of 2 km.

Acknowledgments

- The research has been supported by the Grant Agency of the Czech Republic under Contract P210/10/0736, by the Ministry of Education of the Czech Republic within Research Projects MSM0021620860 and CzechGeo/EPOS LM2010008, and by the members of the consortium "Seismic Waves in Complex 3-D Structures"

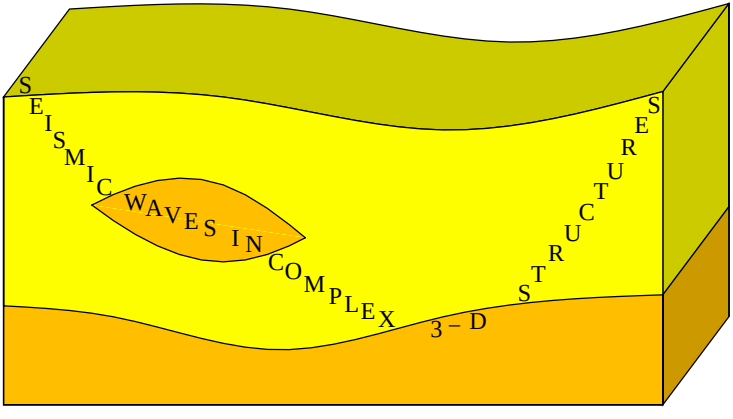

References

Bulant, P. & Klimeš, L. (2015): Nonlinear hypocentre determination. *Seismic Waves in Complex 3–D Structures*, **25**, 17–36, online at "http://sw3d.cz".

Klimeš, L. (1995): Examples of seismic models. *Seismic Waves in Complex 3–D Structures*, **3**, 5–35, online at "http://sw3d.cz".

Klimeš, L. (2002b): Estimating the correlation function of a self–affine random medium. *Pure appl. Geophys.*, **159**, 1833–1853, online at "http://sw3d.cz".